

ANOMALOUS QUARK–GLUON CHROMOMAGNETIC INTERACTION AND HIGH-ENERGY ρ -MESON ELECTROPRODUCTION

N. Korchagin^{a,1}, *N. Kochelev*^{a,2}, *N. Nikolaev*^{b,3}

^a Joint Institute for Nuclear Research, Dubna

^b Forschungszentrum, Institut für Kernphysik, Jülich, Germany

It is shown that existence of a large anomalous chromomagnetic moment of quark induced by nonperturbative structure of QCD leads to the additional contribution to exclusive ρ -meson electroproduction off proton target. The contribution coming from new type of quark–gluon interaction to the ρ -meson production cross section for both transversal and longitudinal polarization of virtual photon is found. Such nonperturbative contribution together with conventional perturbative two-gluon exchange allows us to describe the experimental data at low Q^2 for transversal polarization. However, in the longitudinal polarization case there is still some discrepancy with the data. The possible source of this deviation is discussed.

Показано, что существование большого аномального хромомагнитного момента кварка, индуцированного непертурбативной структурой вакуума КХД, приводит к дополнительному вкладу в эксклюзивное сечение электророждения ρ -мезона на протоне. Найден вклад в сечение рождения при продольной и поперечной поляризации виртуального фотона, идущий от нового типа кварк-глюонного взаимодействия. Такой непертурбативный вклад, вместе с традиционным пертурбативным двухглюонным обменом, позволил нам описать экспериментальные данные при малых Q^2 для поперечной поляризации. Тем не менее в случае с продольной поляризацией все же остается расхождение с данными. Обсуждается возможная причина этого отклонения.

PACS: 24.85.+p; 12.38.-t; 12.38.Mh; 12.39.Mk

INTRODUCTION

One of salient features of perturbative high-energy QCD is conservation of the s -channel helicity of quarks. On the other hand, the QCD vacuum possesses a nontrivial topological structure — instantons are an extensively studied example (for the reviews [1,2]). Such topological fluctuations generate the celebrated multiquark 't Hooft interaction which is responsible, for example, for the solution of $U_A(1)$ problem in QCD [3]. Additionally, instantons were shown to generate a nontrivial spin-flip, i.e., s -channel helicity nonconserving, *quark–gluon*

¹E-mail:kolya.korchagin@gmail.com

²E-mail:kochelev@theor.jinr.ru

³E-mail:n.nikolaev@fz-juelich.de

interaction [4]. This interaction can be described in terms of an anomalous chromomagnetic quark moment (ACQM) complementary to the perturbative Dirac coupling. Novel contributions from this nonperturbative interaction to the soft Pomeron, gluon distribution in the nucleon, and sizable spin effects in strong interactions have already been discussed in the literature [2, 4–6]. A magnitude of the ACQM can be related to the instanton density in the QCD vacuum.

The exclusive vector meson electroproduction is a unique testing ground of the s -channel helicity properties of the quark–gluon coupling. Specifically, s -channel helicity nonconserving transitions from photons to vector mesons are possible even within the perturbative QCD for a fundamental reason that a helicity of mesons can be different from a sum of the quark and antiquark helicities (see [7] and references therein). The ACQM would introduce an extra contribution to both the s -channel helicity conserving and nonconserving vector meson production amplitudes. Although it comes from manifestly soft region, a direct evaluation of such a contribution is needed.

Helicity properties of electroproduced vector mesons have been extensively studied in three experiments at HERA DESY, i.e., by the H1, ZEUS, and HERMES Collaborations. Although gross features of these data are well consistent with pQCD-based theoretical predictions (see review [7] and recent development in [8, 9]), there remain several open issues. An outstanding problem is a large relative phase of the leading helicity amplitudes for production of longitudinal and transverse ρ^0 s and ϕ s, which has been observed by the HERMES and H1 Collaborations [10–12]. It is definitely larger than the prediction based on the handbag mechanism [13] and also in the conventional pQCD pomeron-based color dipole approach [14] (see discussion in [7]). Besides that, pQCD-driven approaches seem to fail with the experimentally observed Q^2 dependence of the ratio σ_L/σ_T in full experimentally studied range of Q^2 : theoretical calculations substantially overestimate this ratio at large Q^2 . Finally, it is important to evaluate an impact of new nonperturbative mechanism on the transition from real to virtual electroproduction.

In the present paper we study exclusive ρ -meson electroproduction off protons with allowance for the novel s -channel helicity nonconservation mechanism induced by the anomalous chromomagnetic moment of quarks. We focus on the simplest observables, σ_L and σ_T , a calculation of the full set of helicity amplitudes will be reported elsewhere.

1. ANOMALOUS QUARK–GLUON CHROMOMAGNETIC INTERACTION

In the most general case, the interaction vertex of massive quark with gluon can be written in the following form:

$$V_\mu(k_1^2, k_2^2, \kappa^2)t^a = -g_s t^a \left[F_1(k_1^2, k_2^2, \kappa^2) \gamma_\mu + \frac{\sigma_{\mu\nu} \kappa_\nu}{2m} F_2(k_1^2, k_2^2, \kappa^2) \right], \quad (1)$$

where the first term is a conventional perturbative QCD quark–gluon vertex and the second term comes from nonperturbative sector of QCD. In Eq. (1) the form factors $F_{1,2}$ describe a nonlocality of the nonperturbative interaction; $k_{1,2}$ are the momenta of incoming and outgoing quarks, respectively, and $\kappa = k_2 - k_1$; m is the quark mass, and $\sigma_{\mu\nu} = (\gamma_\mu \gamma_\nu - \gamma_\nu \gamma_\mu)/2$. In what follows, we focus on effects of the novel color chromomagnetic vertex and keep

$F_1(k_1^2, k_2^2, \kappa^2) = 1$. The anomalous chromomagnetic quark moment equals

$$\mu_a = F_2(0, 0, 0).$$

In the earlier paper [4], it was shown that instantons, a strong vacuum fluctuations of gluon fields with nontrivial topology, generate an ACQM which is proportional to the instanton density

$$\mu_a = -\pi^3 \int \frac{d\rho n(\rho) \rho^4}{\alpha_s(\rho)}.$$

In terms of the average size of instantons ρ_c and the dynamical quark mass m in nonperturbative QCD vacuum one finds [5]

$$\mu_a = -\frac{3\pi(m\rho_c)^2}{4\alpha_s(\rho_c)}, \quad (2)$$

which exhibits a strong sensitivity of the ACQM to a dynamical mass of quarks. To this end, we emphasize an implicit assumption that quarks are light, i.e., the above estimates of ACQM are valid for u, d, s , while for heavy quarks ACQM vanishes. For the average instanton size $\rho_c^{-1} = 0.6$ GeV, this mass is changing from $m = 170$ MeV in the mean field (MF) approximation to $m = 345$ MeV within Diakonov–Petrov (DP) model. The QCD strong coupling constant at the instanton scale can be evaluated as

$$\alpha_s(\rho_c) \approx 0.5,$$

and the resulting ACQM for light quarks is numerically quite large:

$$\mu_a^{\text{MF}} \approx -0.4, \quad \mu_a^{\text{DP}} \approx -1.6.$$

Recently, an ACQM of similar magnitude has been obtained within the Dyson–Schwinger equation approach to nonperturbative QCD (see discussion and references in [15]).

The form factor $F_2(k_1^2, k_2^2, \kappa^2)$ suppresses the ACQM vertex at short distances when the respective virtualities are large. Within the instanton model its explicit form is related to Fourier-transformed quark zero-mode and instanton fields and reads

$$F_2(k_1^2, k_2^2, \kappa^2) = \mu_a \Phi_q(|k_1| \rho/2) \Phi_q(|k_2| \rho/2) F_g(|\kappa| \rho),$$

where

$$\begin{aligned} \Phi_q(z) &= -z \frac{d}{dz} (I_0(z)K_0(z) - I_1(z)K_1(z)), \\ F_g(z) &= \frac{4}{z^2} - 2K_2(z), \end{aligned}$$

where $I_\nu(z)$, $K_\nu(z)$ are the modified Bessel functions and ρ is the instanton size.

Recent discussion has shown [5] that the ACQM contribution complements the pQCD evaluations of the total quark–quark cross section in a way which improves constituent quark model description of high-energy nucleon–nucleon total cross section. Furthermore, such a model provides the soft contribution to the gluon distribution in the nucleon which is consistent with initial conditions to a DGLAP evolution of phenomenological PDFs. A purpose of the present communication is to explore the effects of ACQM in elastic (diffractive) electroproduction of ρ mesons.

2. MODEL FOR VECTOR MESON EXCLUSIVE PRODUCTION

Driven by BFKL considerations, high-energy diffractive production of vector mesons is usually described by an exchange of a color-singlet two-gluon tower in the t channel. The corresponding diagrams are presented in Fig. 1. By using the Sudakov expansion for the momenta of proton and virtual photon

$$p_\mu = p'_\mu + \frac{m_p^2}{s} q'_\mu, \quad q_\mu = q'_\mu - x p'_\mu, \quad q'^2 = p'^2 = 0, \quad (3)$$

where $Q^2 = -q^2$, $x = Q^2/s \ll 1$, $s = 2(p'q')$, the quark momentum k in the quark loop, gluon momentum κ , and momentum transfer to proton Δ (see Fig. 1) can be presented in the following form:

$$\begin{aligned} k_\mu &= y p'_\mu + z q'_\mu + \mathbf{k}_\mu, \\ \kappa_\mu &= \alpha p'_\mu + \beta q'_\mu + \boldsymbol{\kappa}_\mu, \\ \Delta_\mu &= \delta p'_\mu + \sigma q'_\mu + \boldsymbol{\Delta}_\mu, \end{aligned} \quad (4)$$

where any vector \mathbf{l} is a transversal part of four-vector l_μ which satisfies the relation $\mathbf{l} \cdot q' = \mathbf{l} \cdot p' = 0$.

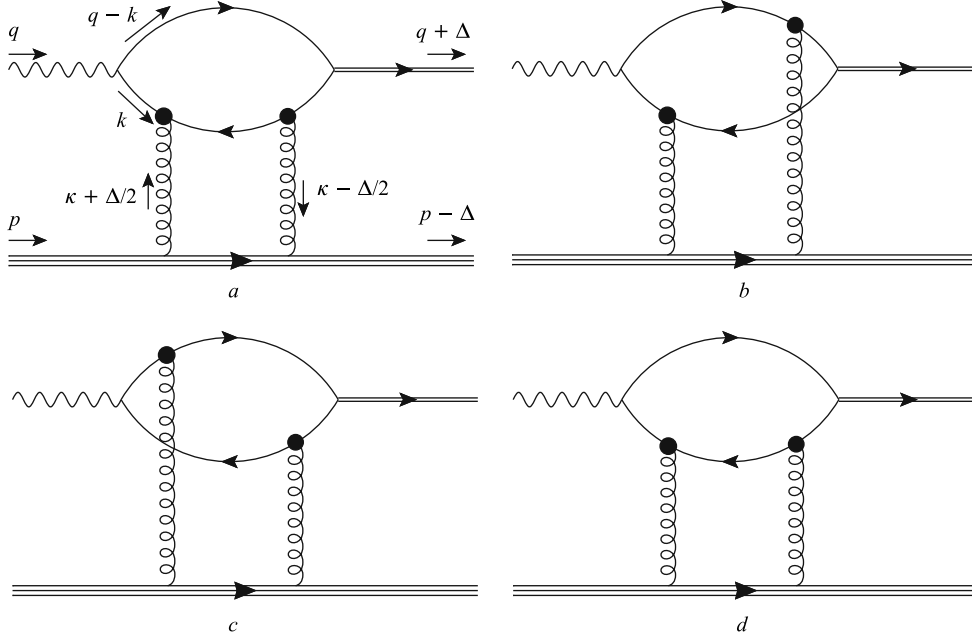


Fig. 1. The diagrams which contribute to high-energy exclusive vector meson electroproduction off proton by two-gluon exchange. Here the blob stands for the generalized quark–gluon vertex (Eq. (1))

Hereafter we follow the k -factorization analysis developed in [16–18]. The polarization vectors for virtual photon e and vector meson V are

$$\begin{aligned} e_{T\mu} &= \mathbf{e}_\mu, & e_{L\mu} &= \frac{1}{Q}(q'_\mu + xp'_\mu), \\ V_{T\mu} &= \mathbf{V}_\mu + \frac{2(\Delta\mathbf{V})}{s}p'_\mu, & V_{L\mu} &= \frac{1}{M}\left(q'_\mu + \frac{\Delta^2 - M^2}{s}p'_\mu + \Delta_\mu\right), \end{aligned} \quad (5)$$

where M is the mass of $\bar{q}q$ pair on mass-shell:

$$M^2 = \frac{\mathbf{k}^2 + m^2}{z(1-z)}. \quad (6)$$

The imaginary part of the amplitude takes the form

$$\begin{aligned} A(x, Q^2, \Delta) &= -is \frac{c_V \sqrt{4\pi\alpha_{\text{em}}}}{4\pi^2} \int \frac{dz}{z(1-z)} \int d^2\mathbf{k} \psi(z, \mathbf{k}) \int \frac{d^2\boldsymbol{\kappa}}{\boldsymbol{\kappa}^4} \alpha_s \mathcal{F}(x, \boldsymbol{\kappa}, \Delta) \times \\ &\times \left[\frac{1-z}{z} \frac{I^{(a)}}{\mathbf{k}_{1a}^2 + m^2 + z(1-z)Q^2} + \frac{I^{(b)}}{\mathbf{k}_{1b}^2 + m^2 + z(1-z)Q^2} + \right. \\ &\left. + \frac{I^{(c)}}{\mathbf{k}_{1c}^2 + m^2 + z(1-z)Q^2} + \frac{z}{1-z} \frac{I^{(d)}}{\mathbf{k}_{1d}^2 + m^2 + z(1-z)Q^2} \right]. \end{aligned} \quad (7)$$

Here α_{em} is the fine-structure constant; $c_V = 1/\sqrt{2}$ is coming from the flavor part of the ρ -meson wave function; $\mathcal{F}(x, \boldsymbol{\kappa}, \Delta)$ is the differential gluon density and $\psi(z, \mathbf{k})$ is light-cone wave function of the ρ meson, for which we use a simple parameterization

$$\psi = c \exp\left(-\frac{a^2 \mathbf{p}^2}{2}\right) = c \exp\left(-\frac{a^2}{2} \left(\mathbf{k}^2 + \frac{1}{4}(2z-1)^2 M^2\right)\right), \quad (8)$$

where \mathbf{p} is 3-dimensional relative momentum of quarks in pair. Two constants a and c were fixed by the normalization of wave function and decay width $\Gamma(\rho \rightarrow e^+e^-)$, we find $a = 3.927 \text{ GeV}^{-1}$, $c = 17.44$.

For the QCD running coupling we use

$$\alpha_s(q^2) = \frac{4\pi}{9 \ln((q^2 + m_g^2)/\Lambda_{\text{QCD}}^2)}, \quad (9)$$

where $\Lambda_{\text{QCD}} = 0.28 \text{ GeV}$, and the value $m_g = 0.88 \text{ GeV}$ imposes the infrared freezing at $\alpha_s(1/\rho_c^2) \approx \pi/6$ [2]. Here q^2 is the maximum virtuality out of momenta which are inserted to vertex, i.e., $q^2 = \max(k_1^2, k_2^2, \kappa^2)$.

$I^{(i)}$ is the trace over quark line in i) diagram from Fig. 1 divided by $2s^2$, it involves three parts:

$$I^{(i)} = I_{\text{pert}}^{(i)} + I_{\text{cm}}^{(i)} + I_{\text{mix}}^{(i)}. \quad (10)$$

Below we are using the following notations for the transverse momentum of quark:

$$\begin{aligned}
 \mathbf{k}_{1a} &= \mathbf{k} - (1 - z)\mathbf{\Delta}, \\
 \mathbf{k}_{1b} &= \mathbf{k} - (1 - z)\mathbf{\Delta} + \boldsymbol{\kappa} + \frac{1}{2}\mathbf{\Delta}, \\
 \mathbf{k}_{1c} &= \mathbf{k} - (1 - z)\mathbf{\Delta} - \boldsymbol{\kappa} + \frac{1}{2}\mathbf{\Delta}, \\
 \mathbf{k}_{1d} &= \mathbf{k} + z\mathbf{\Delta}.
 \end{aligned} \tag{11}$$

Such a shift of momentum is needed for keeping transverse momentum of quarks inserted to meson vertex to be equal to \mathbf{k} for all diagrams in order to take out $\psi(z, \mathbf{k})$ as common multiplier. Besides, $[\mathbf{ab}] = a_x b_y - a_y b_x$.

The formula for TT transition in case when both of quark–gluon vertices are perturbative is

$$I_{\text{pert}}^{(c)}(T \rightarrow T) = [(\mathbf{e}\mathbf{V}^*)(m^2 + \mathbf{k}\mathbf{k}_{1c}) + (\mathbf{V}^*\mathbf{k})(\mathbf{e}\mathbf{k}_{1c})(1 - 2z)^2 - (\mathbf{e}\mathbf{k})(\mathbf{V}^*\mathbf{k}_{1c})]. \tag{12}$$

For pure perturbative vertices there is the relation between different contributions

$$I_{\text{pert}}^{(b)} = I_{\text{pert}}^{(c)} = -\frac{1-z}{z}I_{\text{pert}}^{(a)} = -\frac{z}{1-z}I_{\text{pert}}^{(d)}$$

subject to a proper substitution of the loop quark momenta from the relevant diagrams of Fig. 1.

When both quark–gluon vertices come from nonperturbative ACQM, we find

$$\begin{aligned}
 I_{\text{cm}}^{(a)}(T \rightarrow T) &= -\frac{z}{1-z} [(\mathbf{e}\mathbf{V}^*)(m^2 + \mathbf{k}\mathbf{k}_{1a}) + (\mathbf{V}^*\mathbf{k})(\mathbf{e}\mathbf{k}_{1a})(1 - 2z)^2 - \\
 &\quad - (\mathbf{e}\mathbf{k})(\mathbf{V}^*\mathbf{k}_{1a})] \boldsymbol{\kappa}^2 F_2(k_{\text{I avg}}^2, 0, \boldsymbol{\kappa}^2) F_2(k_{\text{II avg}}^2, 0, \boldsymbol{\kappa}^2). \tag{13}
 \end{aligned}$$

Here we notice that one of quarks is always on mass-shell, and $k_{\text{I,II avg}}^2$ stand for the virtuality of the off-mass shell quark. To obtain formula for $I_{\text{cm}}^{(d)}$ one should perform the substitutions $z/(1-z) \rightarrow (1-z)/z$ and $\mathbf{k}_{1a} \rightarrow \mathbf{k}_{1d}$ in the above expression. The ACQM contribution from the graph in Fig. 1, c is

$$\begin{aligned}
 I_{\text{cm}}^{(c)}(T \rightarrow T) &= \left[((1 - 2z)^2 (\mathbf{V}^*\mathbf{k})(\mathbf{k}_{1c}\mathbf{e}) - (\mathbf{k}\mathbf{k}_{1c})(\mathbf{e}\mathbf{V}^*) + (\mathbf{k}\mathbf{e})(\mathbf{V}^*\mathbf{k}_{1c})) \boldsymbol{\kappa}^2 + \right. \\
 &\quad \left. + m^2 (2(\mathbf{e}\boldsymbol{\kappa})(\mathbf{V}^*\boldsymbol{\kappa}) - (\mathbf{e}\mathbf{V}^*)\boldsymbol{\kappa}^2) \right] F_2(k_{\text{I avg}}^2, 0, \boldsymbol{\kappa}^2) F_2(k_{\text{II avg}}^2, 0, \boldsymbol{\kappa}^2). \tag{14}
 \end{aligned}$$

The replacement $\mathbf{k}_{1c} \rightarrow \mathbf{k}_{1b}$ leads to the formula for $I_{\text{cm}}^{(b)}$.

The interference of the pQCD and ACQM vertices gives

$$\begin{aligned}
 I_{\text{mix}}^{(c)}(T \rightarrow T) &= m [(\mathbf{V}^*\mathbf{k})(\boldsymbol{\kappa}\mathbf{e})(1 - 2z) - [\mathbf{e}\boldsymbol{\kappa}][\mathbf{V}^*\mathbf{k}] - (\mathbf{e}\mathbf{k}_{1c})(\boldsymbol{\kappa}\mathbf{V})(1 - 2z) - \\
 &\quad - [\mathbf{e}\mathbf{k}_{1c}][\boldsymbol{\kappa}\mathbf{V}^*]] (F_2(k_{\text{II avg}}^2, 0, \boldsymbol{\kappa}^2) - F_2(k_{\text{I avg}}^2, 0, \boldsymbol{\kappa}^2)). \tag{15}
 \end{aligned}$$

The $I_{\text{mix}}^{(b)}$ is obtained from the above by substitution $k_{1c} \rightarrow k_{1b}$. The remaining amplitudes are

$$I_{\text{mix}}^{(a)}(T \rightarrow T) = \frac{zm}{1-z} [(\mathbf{V}^* \mathbf{k})(\boldsymbol{\kappa} \mathbf{e})(1-2z) - [\mathbf{e} \boldsymbol{\kappa}][\mathbf{V}^* \mathbf{k}] - (\mathbf{e} \mathbf{k}_{1a})(\boldsymbol{\kappa} \mathbf{V})(1-2z) - [\mathbf{e} \mathbf{k}_{1a}][\boldsymbol{\kappa} \mathbf{V}^*]] (F_2(k_{\text{I avg}}^2, 0, \kappa^2) - F_2(k_{\text{I avg}}^2, 0, \kappa^2)), \quad (16)$$

$$I_{\text{mix}}^{(d)}(T \rightarrow T) = \frac{(1-z)m}{z} [(\mathbf{V}^* \mathbf{k})(\boldsymbol{\kappa} \mathbf{e})(1-2z) + [\mathbf{e} \boldsymbol{\kappa}][\mathbf{V}^* \mathbf{k}] - (\mathbf{e} \mathbf{k}_{1d})(\boldsymbol{\kappa} \mathbf{V}^*)(1-2z) + [\mathbf{e} \mathbf{k}_{1d}][\boldsymbol{\kappa} \mathbf{V}^*]] (F_2(k_{\text{I avg}}^2, 0, \kappa^2) - F_2(k_{\text{I avg}}^2, 0, \kappa^2)). \quad (17)$$

For the longitudinal polarization we obtain

$$I_{\text{pert}}^{(c)}(L \rightarrow L) = -4QMz^2(1-z)^2, \quad (18)$$

$$I_{\text{cm}}^{(c)}(L \rightarrow L) = -4QMz^2(1-z)^2 \kappa^2 F_2(k_{\text{I avg}}^2, 0, \kappa^2) F_2(k_{\text{I avg}}^2, 0, \kappa^2).$$

And $I^{(b)} = I^{(c)} = -\frac{1-z}{z} I^{(a)} = -\frac{z}{1-z} I^{(d)}$ with corresponding \mathbf{k}_{1i} . In the longitudinal case the contribution from the interference of pQCD and ACQM vertices vanishes

$$I_{\text{mix}}^{(a)}(L \rightarrow L) = I_{\text{mix}}^{(b)} = I_{\text{mix}}^{(c)} = I_{\text{mix}}^{(d)} = 0. \quad (19)$$

A common feature of nonperturbative approaches is a fast running dynamical mass of constituent quarks which drops to a small current quark mass at large virtualities. In principle, the running of the quark masses affects the Q^2 dependence of vector meson production observables. However, such a full-fledged involved calculation is beyond the scope of the present communication. Here we only recall that according to the color transparency considerations the vector meson production amplitudes are dominated by the components of the vector meson wave function taken at transverse size, i.e., the scanning radius $r_S \sim 6/\sqrt{Q^2 + m_V^2}$ [7,19,20]. Consequently, the virtuality of quarks is $\propto (Q^2 + m_V^2)$, and arguably one can model an approach to the pQCD regime at large virtuality of the photon making use of a simple approximation

$$m(Q^2) = \frac{m(0)}{1 + Q^2/m_V^2}, \quad (20)$$

where $m(0) = 345$ MeV and $m_V = 770$ MeV.

3. DISCUSSION OF THE RESULTS FOR σ_L AND σ_T

The final result for cross sections is presented in Fig.2 in comparison with data obtained by H1 and ZEUS Collaborations. Helicity flip transitions are found to give a very small contribution to the total production cross section, see also discussion in [7]:

$$\sigma_T = \sigma_{T \rightarrow T} + \sigma_{T \rightarrow L} \approx \sigma_{T \rightarrow T}, \quad (21)$$

$$\sigma_L = \sigma_{L \rightarrow L} + \sigma_{L \rightarrow T} \approx \sigma_{L \rightarrow L}.$$

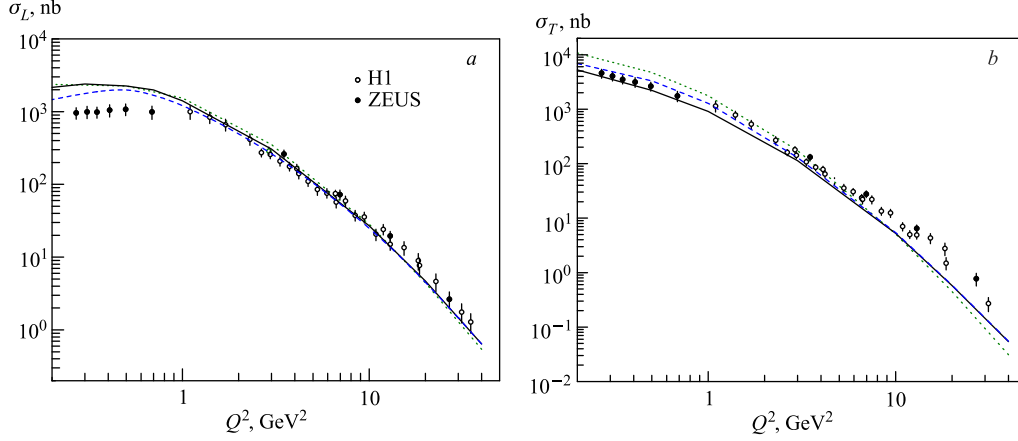


Fig. 2. Cross sections of ρ -meson exclusive electroproduction: *a*) for longitudinal virtual photon polarization; *b*) for transversal photon polarization. The solid line is the calculation with ACQM, dashed line is the result of pQCD contribution with running quark mass, Eq.(20), and dotted line is pQCD calculation with fixed quark mass $m_q = 220$ MeV [17,18]. Experimental points are taken from [21] for H1 and from [22] for ZEUS Collaborations

The longitudinal cross section σ_L is free of the interference of the pQCD and ACQM vertices. Allowance for ACQM effects slightly enhances σ_L in the region of nonperturbative small Q^2 , but still the cross section is overestimated in low Q^2 region. There is one caveat, though: we evaluated the pQCD contribution using the unintegrated gluon density which has been tuned to the experimental data on the proton structure function. To be more accurate, one must reanalyze the structure function data with allowance for the ACQM effect, arguably that would lower somewhat the resulting pQCD contribution to σ_L bringing the theoretical curve closer to the experimental data points.

The case of the transverse cross section σ_T is more subtle. In this case the effect of the pQCD–ACQM interference is quite substantial. As a matter of fact, the resulting destructive interference numerically takes over the pure ACQM contribution and lowers σ_T compared to the pure pQCD contribution. It is well understood that σ_T is more susceptible to the nonperturbative effects in comparison with σ_L . Indeed, the nonperturbative corrections to σ_T die out substantially slower than corrections to σ_L .

To this end we notice that we only treated a leading in $1/N_c$ restricted class of the instanton induced nonperturbative QCD interactions which are reducible to the anomalous chromomagnetic quark–gluon vertex. The full-fledged 't Hooft-like multipartonic interaction [3] gives rise to the more complicated diagrams, examples are shown in Fig. 3. The issue of such contributions will be considered elsewhere [23]. We also have checked the possible effect of introduction of the form factor into pQCD vertex which cuts low transfer momentum region where one-gluon exchange picture looks questionable. It leads to the decreasing of both the longitudinal and the transverse cross sections at low Q^2 . In this case we observe significant improvement of agreement with experiment of our calculation for σ_L , but agreement of calculated σ_T with data becomes worse.

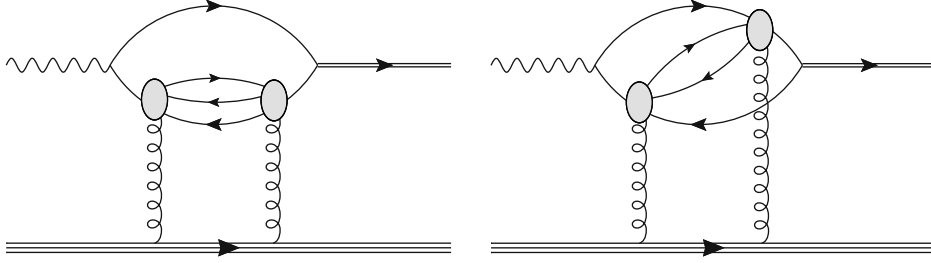


Fig. 3. Additional contribution to exclusive electroproduction of the ρ meson coming from quark-antiquark exchange between chromomagnetic vertices

As we emphasized, the ACQM vertex manifestly violates the quark s -channel helicity conservation. Arguably, the effects of ACQM will be stronger in the helicity flip amplitudes of vector meson electroproduction. The numerical results for full spin density matrix of diffractive ρ mesons will be presented elsewhere.

Acknowledgements. The authors are very grateful to I. O. Cherednikov, A. E. Dorokhov, E. A. Kuraev, and L. N. Lipatov for useful discussions. This work was supported in part by RFBR grant 10-02-00368-a, by Belarus–JINR grant, and by Heisenberg–Landau programme.

REFERENCES

1. Schäfer T., Shuryak E. V. // *Rev. Mod. Phys.* 1998. V. 70. P. 1323.
2. Diakonov D. // *Prog. Part. Nucl. Phys.* 2003. V. 51. P. 173.
3. 't Hooft G. // *Phys. Rev. D.* 1976. V. 32. P. 3432.
4. Kochelev N. I. // *Phys. Lett. B.* 1998. V. 426. P. 149.
5. Kochelev N. Role of Anomalous Chromomagnetic Interaction in Pomeron and Odderon Structures and in Gluon Distribution // *Part. Nucl., Lett.* 2010. V. 7. P. 326; arXiv:0907.3555 [hep-ph].
6. Kochelev N. I. hep-ph/9707418.
7. Ivanov I. P., Nikolaev N. N., Savin A. A. Diffractive Vector Meson Production at HERA: From Soft to Hard QCD // *Part. Nucl.* 2006. V. 37. P. 1.
8. Anikin I. V. et al. // *Phys. Rev. D.* 2011. V. 84. P. 054004; arXiv:1105.1761 [hep-ph].
9. Anikin I. V. et al. // *Nucl. Phys. B.* 2010. V. 828. P. 1; arXiv:0909.4090 [hep-ph].
10. Airapetian A. et al. (HERMES Collab.). Spin Density Matrix Elements in Exclusive ρ^0 Electroproduction on 1H and 2H Targets at 27.5 GeV Beam Energy // *Eur. Phys. J. C.* 2009. V. 62. P. 659; arXiv:0901.0701 [hep-ex].
11. Augustyniak W., Borissov A., Manayenkov S. I. Spin Density Matrix Elements from Diffractive ϕ -Meson Production at HERMES. arXiv:0808.0669 [hep-ex].
12. Adloff C. et al. (H1 Collab.). Elastic Electroproduction of ρ Mesons at HERA // *Eur. Phys. J. C.* 2000. V. 13. P. 371.
13. Goloskokov S. V., Kroll P. The Role of the Quark and Gluon GPDs in Hard Vector–Meson Electroproduction // *Eur. Phys. J. C.* 2008. V. 53. P. 367.

14. *Nemchik J. et al.* Color Dipole Phenomenology of Diffractive Electroproduction of Light Vector Mesons at HERA // *Z. Phys. C.* 1997. V. 75. P. 71.
15. *Chang L., Roberts C.D., Tandy P.C.* Selected Highlights from the Study of Mesons. arXiv:1107.4003[nucl-th].
16. *Kuraev E.V., Nikolaev N.N., Zakharov B.G.* Diffractive Vector Mesons beyond the s-Channel Helicity Conservation // *JETP Lett.* 1998. V. 68. P. 696–703; hep-ph/9809539.
17. *Ivanov I.P., Nikolaev N.N.* Deep-Inelastic Scattering in k Factorization and the Anatomy of the Differential Gluon Structure Function of the Proton // *Phys. At. Nucl.* 2001. V. 64. P. 753; *Phys. Rev. D.* 2002. V. 65. P. 054004.
18. *Ivanov I.P.* Diffractive Production of Vector Mesons in Deep Inelastic Scattering within $k(t)$ Factorization Approach. arXiv:hep-ph/0303053.
19. *Nikolaev N.N.* // *Comments Nucl. Part. Phys.* 1992. V. 21. P. 41.
20. *Kopeliovich B.G. et al.* // *Phys. Lett. B.* 1993. V. 309. P. 179.
21. *Aaron F.D. et al. (H1 Collab.).* Diffractive Electroproduction of ρ and ϕ Mesons at HERA // *JHEP.* 2010. V. 1005. P. 032; arXiv:0910.5831 [hep-ex].
22. *Clerbaux B.* Elastic Production of Vector Mesons at HERA: Study of the Scale of the Interaction and Measurement of the Helicity Amplitude. arXiv:hep-ph/9908519.
23. *Korchagin N., Kochelev N., Nikolaev N.* In preparation.

Received on March 1, 2012.